Proceedings of the European Control Conference 2007
Kos, Greece, July 2-5, 2007

Experimental testing and modelling of a passive mechanical steering compensator for high-performance motorcycles

Christakis Papageorgiou, Oliver G. Lockwood, Neil E. Houghton and Malcolm C. Smith

Abstract— **This paper presents experimental results and a modelling study of a prototype mechanical device that represents a novel steering compensator for high-performance motorcycles. The mechanical device is different from conventional damper devices since it has been designed to represent a series combination of a damper and an inerter. The ideal inerter is a one-port mechanical element which is the exact analogue of the capacitor under the force-current analogy between mechanical and electrical networks, so that the force (torque) through the device is proportional to the relative acceleration (angular acceleration) across its terminals. The steering compensator is tested on a hydraulic test rig and the experimental admittance of the device is calculated over a specified frequency range. A model of the device is developed, including parasitic effects and nonlinearities, which achieves a good fit between model and experimental data.**

I. Introduction

This paper explores some of the practical issues involved in an approach to mechanical control based on the synthesis of passive mechanical networks. The specific context is the application of the method to the control of motorcycles steering instabilities. Simulation studies have shown the potential for significant improvements in weave and wobble instabilities [1], [2]. The following questions naturally arise. Can a device with reasonable physical constraints be constructed to achieve this form of mechanical control? Can the required frequency response characteristics be achieved in practice? What is the nature of the deviations from ideal behaviour? This paper examines these questions for a first prototype device which has been constructed for this application.

II. Preliminaries

A. The inerter

A new mechanical network element termed the "inerter" was recently introduced as an alternative to the mass element for *synthesis* of mechanical networks [3]. In the context of vehicle suspensions this was exploited in [4] by optimizing standard performance measures over low-order fixed-structure admittances and in [5] by optimizing the same performance measures over arbitrary positive real admittances using matrix inequalities. In both cases it was verified that the use of the inerter resulted in considerable improvements in ride comfort, tire grip and handling.

The inerter is a mechanical two-terminal device with the property that the equal and opposite force applied at the two terminals is proportional to the *relative* acceleration between the terminals. Both terminals should be independently movable. The inerter is in fact completely analogous to the capacitor, in the force-current analogy, whereas the mass element is analogous only to a grounded capacitor. The equation for the *ideal* inerter is given by,

$$F = b(\dot{v}_2 - \dot{v}_1) \tag{1}$$

where F is the force applied at the terminals, v_1, v_2 are the velocities of the terminals and b is a constant of proportionality called the inertance which has units of kilograms. The admittance of a mechanical one-port network is defined as the ratio of Laplace transforms of the force over the relative velocity of its terminals. Therefore, the admittance function of the ideal inerter is given by $Y(s) = bs$.

Various physical realizations of the ideal inerter have been described in [3] and [6]. Such a realization may be viewed as approximating its mathematical ideal in the same way that real springs, dampers, capacitors etc approximate their mathematical ideals. Two prototype inerter devices have been manufactured in the Cambridge University Engineering Department (CUED) workshops. The first is a rack-and-pinion inerter and the second is a ballscrew inerter. In the first device the relative translation of the terminals is transduced into a rotation of the flywheel using a rack, pinion and gears while in the second device a ballscrew mechanism is used. These devices have been tested on a hydraulic test rig and it was verified that over a useful frequency range the experimental admittance function is approximately the same as the theoretical admittance function. The results from the testing of these translational devices are presented in more detail in [7]. In this paper we are considering a rotational mechanical device which is designed to act as a series network of an inerter and a damper.

B. Motorcycle steering compensators

There exist two significant steering instabilities associated with motorbikes called "weave" and "wobble" [1]. The weave mode is an oscillatory fish-tailing type of motion that involves rolling and yawing of the whole motorbike body and lateral movements of the steering system. It is a low frequency oscillation typically in the range of 2–4 Hz and it becomes increasingly less damped and possibly unstable at high speeds. Wobble is an oscillation mainly involving

This work was supported in part by EPSRC and DTI

C. Papageorgiou papageorgiou@isy.liu.se is a researcher in the Automatic Control group at the University of Linkoping, Linkoping 581 83, Sweden.

N. E. Houghton neh27@cam.ac.uk and M. C. Smith mcs@eng.cam.ac.uk are with the Department of Engineering, University of Cambridge, Cambridge CB2 1PZ, UK

O. G. Lockwood was an M.Eng student in the Department of Engineering, University of Cambridge, Cambridge CB2 1PZ, UK in 2005–6

ISBN: 978-960-89028-5-5

Fig. 1. The steering compensator device

the steering system and is typically in the frequency range of 6–9 Hz. It is mainly a problem at low speeds although there have been accounts of high-speed wobble oscillations. A more detailed description of these modes is given in [8], where the authors present the effect of regular road forcing on the steering system of a motorcycle and give explanations for various serious motorbike accidents involving these oscillatory modes.

It turns out that a conventional steering damper tends to dampen the wobble mode while at the same time destabilising the weave mode. When the inerter was considered as a steering compensator in [2] it was found to dampen the weave mode but to reduce the stability of the wobble mode. It was therefore proposed to design a passive mechanical network that would contain a damper, an inerter and possibly a spring connected in such way so that the network would act as an inerter at the weave frequencies and as a damper at the wobble frequencies. Various networks based around the simple scheme of a series combination of a damper and an inerter were shown to be advantageous using an advanced motorcycle simulation model [2].

C. The prototype motorcycle steering compensator

A prototype steering compensator was manufactured in the Cambridge University Engineering Department workshops to investigate the more practical mechanical design issues following the work of [2]. The question is addressed of whether it is possible to approximate the theoretical admittance function of an ideal steering compensator, such as the one suggested in [2], subject to size and weight constraints and in the presence of other nonlinear characteristics such as backlash and friction. The prototype steering compensator device is shown in Fig. 1. It has a mass of 1.48 kg, maximum instantaneous torque rating of 60 Nm, length 187 mm and diameter 71 mm. It consists of an epicyclic gearbox (50:1 ratio) driven by a lever arm of length 50 mm. The output side of the gear box is connected to a disc of relatively small inertia which gives rise to a parasitic inertance component as will be described later. Between the disc and the flywheel, which are both located inside the cylindrical casing shown in Fig. 1, there is a small clearance which is occupied by oil. The oil is responsible for transferring torque from the disc to the main flywheel, which accounts for the main inertance of the device. Oils of different viscosity can be used in order to either increase or reduce the damping. Apart from the inertance and the damping, there is a spring effect associated with the device due to the elasticity of the gearbox. Although the device is rotational, we will consider it as being a translational device in the subsequent analysis. The translational inertance, damper rate and spring rate are given by their rotational counterparts scaled by the inverse of the lever arm squared ($\frac{1}{0.05^2}$).

III. Experimental procedure

A. The hydraulic test rig

A Schenck hydraulic rig was used to test the steering compensator. The displacement of the hydraulic ram is controlled in closed-loop with a PID controller and the device to be tested can be placed between the hydraulic ram and a fixed point directly above it. The hydraulic rig regulates the oil flow in the chambers of a cylinder in order to move the ram according to the demands of the control system. The control instrumentation consists of a PID controller and a power amplifier that drives the servo-valve. There are sensors which provide measurements of the ram displacement, the input current to the servo-valve and the load force on the mechanical specimen that is being tested. The measurements are filtered with analogue filters and logged using a data acquisition module. The demanded displacement is generated by a dSPACE processor interfacing with a Simulink application and is fed as an external input to the PID controller. Since the steering compensator is a rotational device, a driving rod and a short lever arm were designed to transduce the linear motion of the hydraulic ram into a rotational motion of the gearbox. The experimental set-up is shown in Fig. 2.

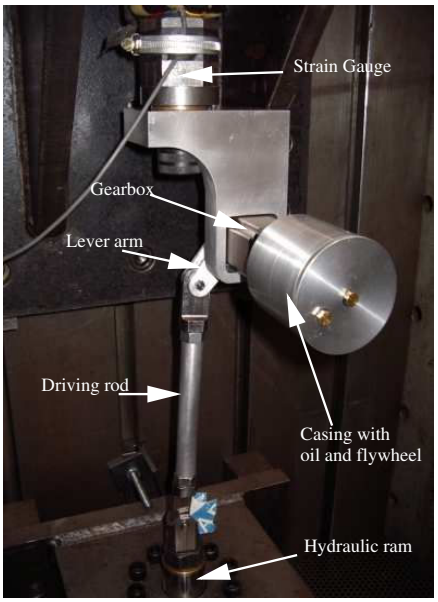

Fig. 2. The steering compensator on the hydraulic test rig

The identification procedure for the calculation of the admittance of the device involves the excitation of the demanded displacement with sinusoidal signals in an appropriate frequency range. At each frequency measurements

of the demanded displacement, the actual ram displacement and the force through the device are recorded. Using the correlation method [9, p.143] the gain and phase of the transfer function from the demanded displacement to the actual ram displacement ($\hat{x}/\hat{x}_{dem}$) and the force respectively ($\hat{F}/\hat{x}_{dem}$) are calculated (where $\hat{}$ denotes Laplace transform). The experimental estimate of the admittance function $\hat{F}/(s\hat{x})$ of the device is then deduced directly from this pair of gain and phase estimates.

B. Experimental results

The experimental admittance of the steering compensator was calculated for four different oils using 33 logarithmically spaced frequency points in the range $[0.1, 35]$ Hz. The admittance function for each oil is shown in Fig. 3. The

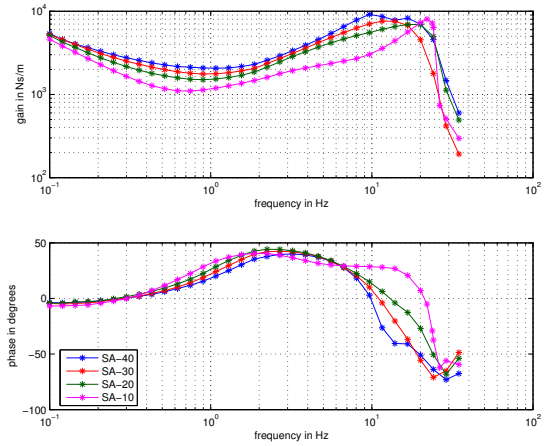

Fig. 3. The experimental admittance functions for different types of oil.

SAE-40 oil has the largest viscosity while the SAE-10 oil has the smallest viscosity. It is encouraging that for all oil types the admittance function has a positive phase for a certain frequency range which is expected due to the presence of an inerter. Note that there is a steep gain roll-off at high frequencies and a corresponding negative phase for all four oils. Such an effect was anticipated due to compliance (flexibility) in the gearbox casing and will be modelled in the next section by a series spring. In all four cases two nonlinear characteristics are also observed in the admittance functions. At low frequencies there is a falling gain characteristic as a function of frequency while the phase remains constant at a negative value close to zero degrees. At high frequencies the gain rolls off at a rate of more than 20 dB/dec while the phase does not go below -90^o. We will demonstrate in the next section that these characteristics can be accounted for by friction and backlash respectively.

IV. Modelling of the Device

A. Ideal linear model

The experimental admittance functions were initially compared to those of an ideal linear model consisting of an inerter in series with a damper together with two parasitic effects: a parallel inertance associated with the gearbox output shaft and disc, and a series spring associated with gearbox compliance. This model is illustrated in Fig. 4. The

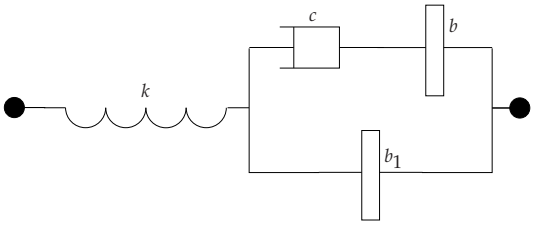

Fig. 4. The linear model of the steering compensator

admittance of this linear network is given by

$$Y(s) = \frac{kbb_1s^2 + kc(b+b_1)s}{bb_1s^3 + c(b+b_1)s^2 + kbs + kc}. \qquad (2)$$

We see that if there is no oil in the cylinder ($c = 0$), then only the disc rotates and the admittance becomes $ks/(s^2 + k/b_1)$ which has a resonance at a frequency of $\sqrt{k/b_1}$ rad/s. If the oil has very large viscosity ($c \to \infty$), then we effectively have two inerters in parallel and the admittance becomes $ks/(s^2 + k/(b+b_1))$ with a resonance at the smaller frequency of $\sqrt{k/(b+b_1)}$ rad/s. A family of frequency responses showing the transition from one resonant peak to the other as the damper rate c varies is given in Fig. 5 (with k, b, b_1 chosen as Table I). The figure shows a frequency for which the gain

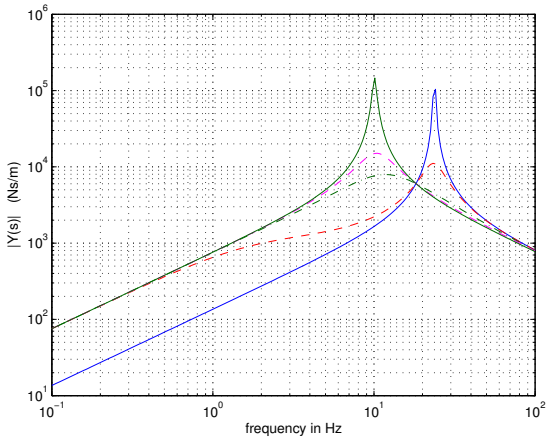

Fig. 5. The gain of the theoretical admittance function Y(s) as a function of c.

of $Y(s)$ does not change with respect to c. It can be verified analytically that this frequency is given by $\sqrt{\frac{1}{2}\left(\frac{k}{b_1} + \frac{k}{b+b_1}\right)}$.

During the mechanical design phase of the steering compensator the various parameters in the linear model of Fig. 4 were either chosen or estimated to have the values shown in Table I. The corresponding admittance function $Y(s)$ is illustrated in Fig. 6 for the four oils.

A comparison of Figs. 6 and 3 shows a broad similarity between the experimental and theoretical responses in the middle frequency range. This suggested that the prototype

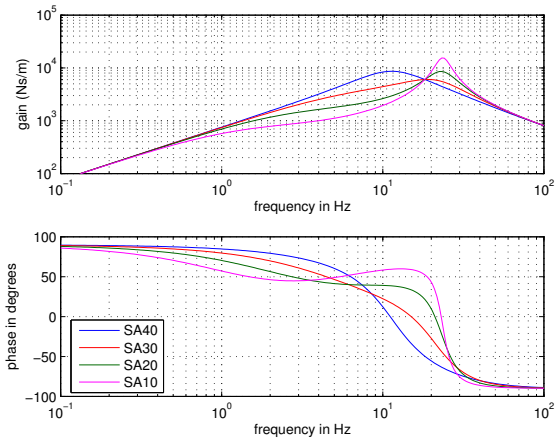

Fig. 6. The theoretical admittance function Y(s) for the parameters given in Table I.

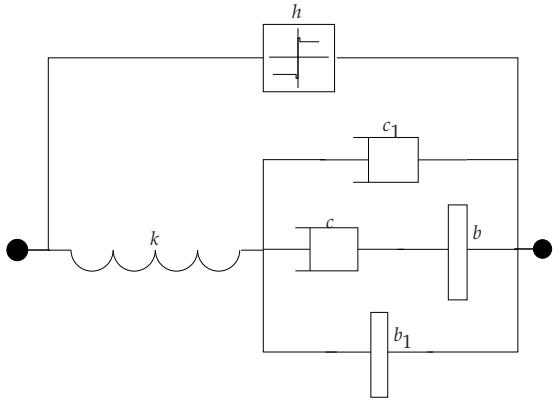

Fig. 7. The augmented nonlinear model of the steering compensator

was functioning as anticipated and that the linear model of Fig. 4 was a sensible initial choice.

B. Friction modelling

To properly model the behaviour of the device at low frequencies a friction model was needed. Bench measurements on the gear box indicated linear friction equivalents as follows: static friction $f_s = 2$ N and dynamic friction $f_d = 1.75$ N. Initial attempts at parameter fitting did not succeed in achieving a sufficiently close match between experimental admittance function and model. Accordingly it was decided to introduce an additional linear damping term in parallel with the parasitic inertance as well. This gave rise to the model illustrated in Fig. 7 which is used for parameter estimation in this section. The actual friction forces in the model are assumed to be $\pm 2h$ N and $\pm 1.75h$ N where the parameter h is a variable, and the additional linear damper is c_1.

To estimate the nonlinear model parameters the following criterion was considered:

$$J_{\text{oil}} = \sum_{i=1}^{n_f} \frac{|Y(p, j\omega_i) - E_{\text{oil}}(j\omega_i)|}{|E_{\text{oil}}(j\omega_i)|} \qquad (3)$$

in which n_f is the number of frequency points, the decision variable is given by $p = [c, c_1, h, k, b_1, b]$ and $E_{\text{oil}}(j\omega_i)$ is the experimental admittance function corresponding to a specific oil (oil=SAE10, SAE20 etc). The term $Y(p, j\omega_i)$ is the admittance function which is calculated from the nonlinear model using the frequency correlation method and the same excitation inputs as the ones used for the calculation of the experimental admittance functions. The optimization was solved using the Matlab function *fmincon* and initially only the frequencies from 0.1 Hz to 20 Hz were considered in order to disregard any backlash related effects. It was assumed that the parameters h, k, b and b_1 were the same independent of the type of oil used in the compensator. The optimization was performed in two steps:

- **Step 1:** Assume constant values for c and c_1 for the four types of oil and choose h, k, b_1 and b in order to minimise $J_t = J_{\text{SAE10}} + J_{\text{SAE20}} + J_{\text{SAE30}} + J_{\text{SAE40}}$.
- **Step 2:** Use the values of h, k, b_1 and b from step 1 and optimise J_{oil} over c and c_1 for the four types of oil.

The results of the optimization are presented in Figs. 8-11 for each type of oil. The model parameters are presented in Table II. We observe that for all oils there is a good agreement in the magnitude of the experimental and the model admittances especially in the frequency range [0.1-10] Hz. Evidently the falling gain characteristic at low frequencies is well modelled by the friction and parasitic damping though there is still a small phase error at low frequencies which will be addressed later on. Comparing the estimated parameter values of Table II with the expected design parameters of Table I we observe only small differences in the main and parasitic inertances and the spring stiffness of the gearbox. The estimated values for the main damper rates are fairly different from their intended design values. Also the estimated friction is higher than suggested by the bench measurements by a factor of 9.36. After the experiments were completed the device was partially disassembled to investigate the source of the increased friction. It was found that a small clearance error had given rise to this increased friction in the fully assembled device which could be easily corrected.

TABLE I

THE DESIGN PARAMETERS OF THE STEERING COMPENSATOR

Parameter	Linear equivalent value	
k	480 kN/m	
b	98.4 kg	
b_1	21.6 kg	
c	5518 Ns/m	SAE-40
	2759 Ns/m	SAE-30
	1380 Ns/m	SAE-20
	690 Ns/m	SAE-10

C. Inclusion of a backlash model in the steering compensator

The model of the steering compensator was further augmented by including a rotational backlash model in the

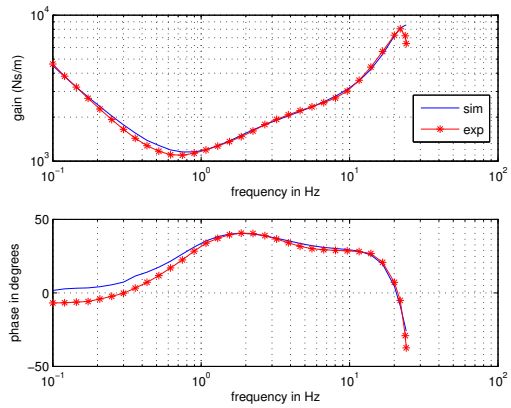

Fig. 8. The experimental and theoretical admittance function for the SAE-10 oil.

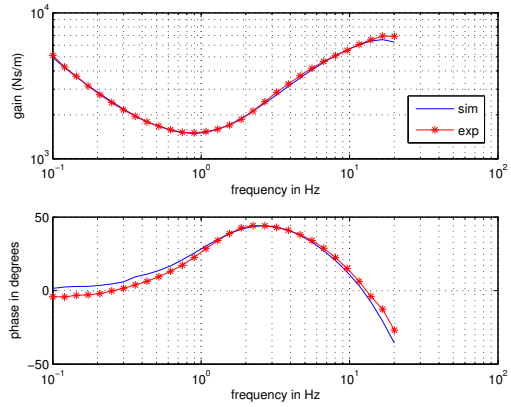

Fig. 9. The experimental and theoretical admittance function for the SAE-20 oil.

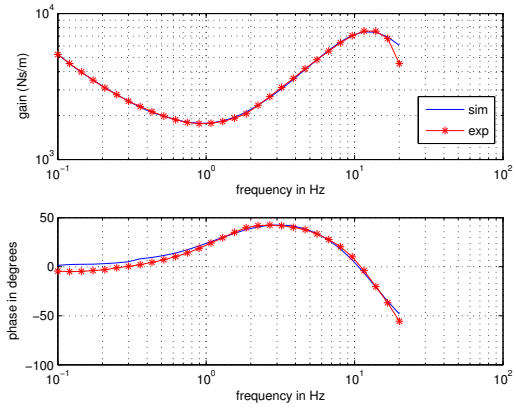

Fig. 10. The experimental and theoretical admittance function for the SAE-30 oil.

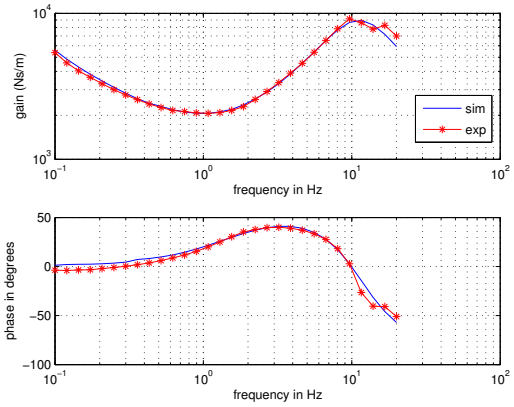

Fig. 11. The experimental and theoretical admittance function for the SAE-40 oil.

gearbox. The backlash model was taken from [10] and consists of an inertia-free shaft with a backlash gap 2α rad, and a spring with elasticity $k_{b,\mathrm{rot}}$ (Nm/rad) in parallel with a viscous damping $c_{b,\mathrm{rot}}$ (Nms/rad) as shown in Fig. 12. The

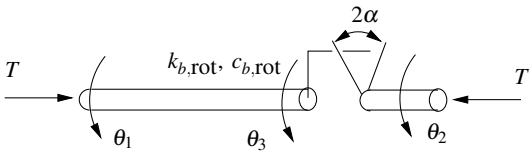

Fig. 12. Schematic of the backlash model

equivalent translational parameter c_b for the shaft damper rate was set to 100 Ns/m while the translational spring constant k_b is assumed to correspond to the translational value of the flexibility of the gearbox as mentioned previously. The steering compensator model including the backlash is shown in Fig. 13.

The same cost function and the same optimization procedure was used for the estimation of the model parameters although we maintain the friction parameter h constant at $h = 9.36$ since the friction only affects the low frequency characteristic. The decision variable is now given by $p = [c, c_1, k, b_1, b, \alpha]$. For the optimisation, the displacement excitation given to the model is the same as the displacement levels used in the experiments since backlash behaviour is

TABLE II

THE ESTIMATED PARAMETERS FOR THE FRICTION MODEL OF THE STEERING COMPENSATOR

Parameter	Linear equivalent value	
k	563 kN/m	
b	94.5 kg	
b_1	23 kg	
h	9.36	
c, c_1	[5742,1430] Ns/m	SAE-40
	[4346,1100] Ns/m	SAE-30
	[3219,780] Ns/m	SAE-20
	[1472,347] Ns/m	SAE-10

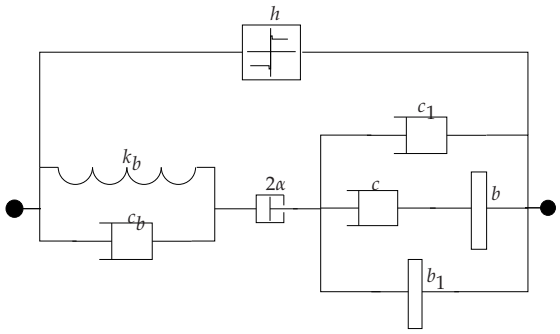

Fig. 13. The model of the steering compensator with friction and backlash.

TABLE III
THE ESTIMATED PARAMETERS FOR THE BACKLASH MODEL OF THE STEERING COMPENSATOR

Parameter	**Run 1,** $f_{max} = 24$ **Hz**	**Run 2,** $f_{max} = 36$ **Hz**
k_b	875 kN/m	861 kN/m
b	81.2 kg	80.1 kg
b_1	24.4 kg	24.8 kg
α	0.00338 rad	0.00336 rad
c, c_1	[6382,1398] Ns/m	[6261,1397] Ns/m SAE-40
	[4423,1104] Ns/m	[4349,1106] Ns/m SAE-30
	[3062,804] Ns/m	[3035,808] Ns/m SAE-20
	[1375,364] Ns/m	[1354,370] Ns/m SAE-10

largely dependent on the level of external displacement.

Two different optimization runs with the backlash model of the steering compensator were carried out. The first run considers frequency points up to a frequency of 24 Hz while the second run considers frequency points up to 36 Hz. The estimated parameter values for the two runs are shown in Table III. We see that the values of the parameters for the two runs are fairly similar. In both cases the spring stiffness value is considerably larger than the one predicted without the backlash model (see Table II). Also the main inertance value is lower. The experimental and theoretical admittance functions corresponding to the estimated parameters of run 2 are shown in Figs 14–17. There is a very good fit in the

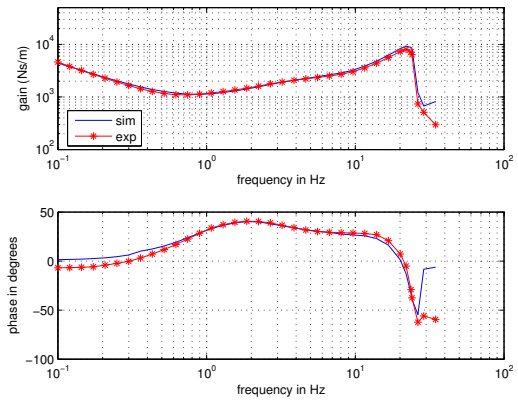

Fig. 14. The experimental and theoretical admittance function for the SAE-10 oil.

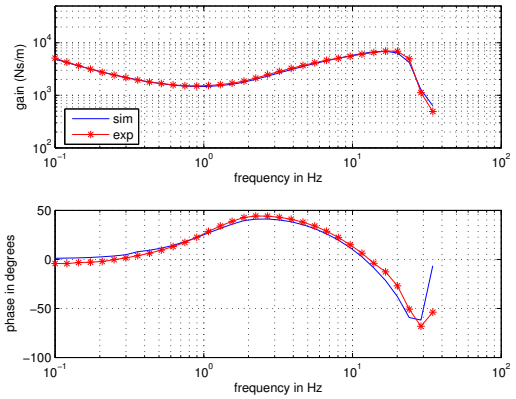

Fig. 15. The experimental and theoretical admittance function for the SAE-20 oil.

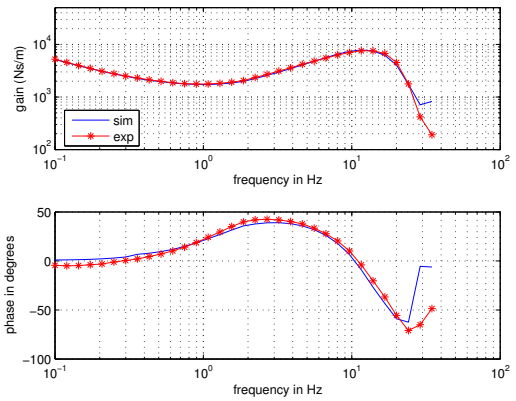

Fig. 16. The experimental and theoretical admittance function for the SAE-30 oil.

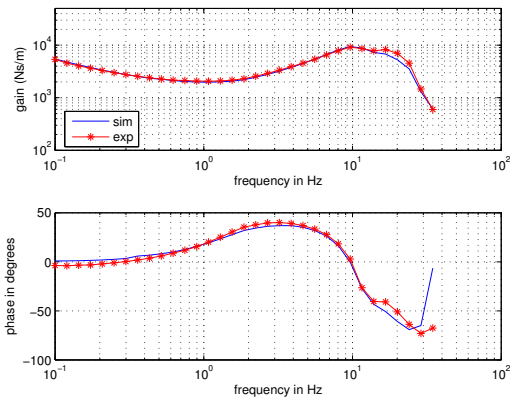

Fig. 17. The experimental and theoretical admittance function for the SAE-40 oil.

gain characteristic for each oil but there is discrepancy in the high frequency phase characteristic. The estimated rotational backlash value is 0.39^o which corresponds to 0.34 mm of translational backlash. The manufacturer's upper bound estimate for the backlash in the gearbox was 0.083^o. After the experiments were completed the device was dismantled and the backlash in the gearbox was measured directly on the bench. The value obtained was 0.092^o. The time-domain experimental data was also carefully examined and shown to be consistent with the larger backlash estimate of 0.39^o. It was therefore concluded that the increased backlash must be accounted for in the joints of the connecting pieces or in the keying.

D. Comparison of experimental and theoretical time responses

In this section we present a brief comparison between the theoretical and the experimental time responses for the SAE-10 oil. We compare the time responses at four frequency points namely, $f = 0.1$, 3.2, 8 and 20 Hz. The comparison is presented in Figs 18–21. The theoretical and experimental time responses agree fairly well for the four frequencies. There is a small phase discrepancy at $f = 0.1$ Hz which will be discussed in the next section.

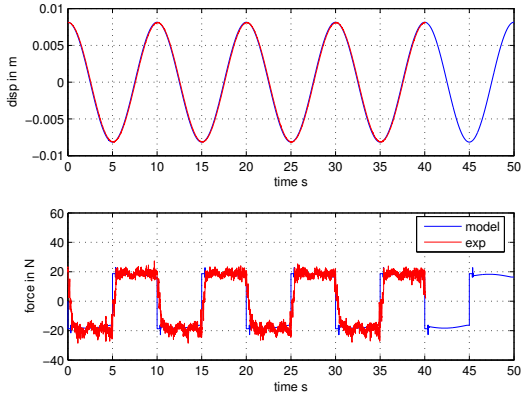

Fig. 18. Comparison of theoretical and experimental time responses at $f = 0.1$ Hz.

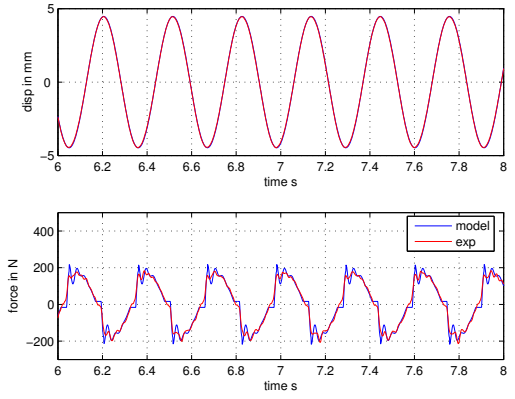

Fig. 19. Comparison of theoretical and experimental time responses at $f = 3.2$ Hz.

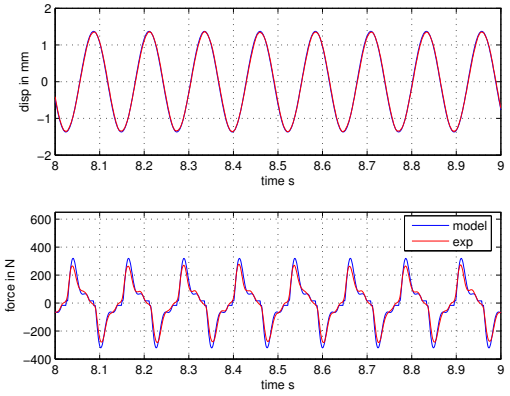

Fig. 20. Comparison of theoretical and experimental time responses at $f = 8$ Hz.

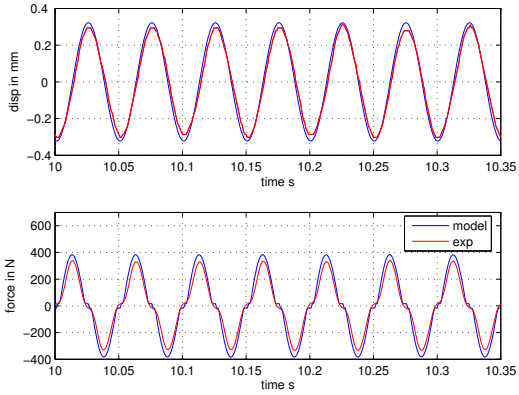

Fig. 21. Comparison of theoretical and experimental time responses at $f = 20$ Hz.

E. Refinement of the friction model

Although the existing friction model can predict very well the falling gain characteristic at low frequencies, it fails to capture the small negative phase behaviour at low frequencies. For this reason the time-domain force-velocity characteristic for the SAE-10 oil at $f = 0.1$ Hz was examined for further clues and is shown in Fig. 22. At this low frequency the measured force is mainly affected by the friction in the device. We see that contrary to the existing friction model, the force-velocity characteristic has a hysteretic behaviour which results in the force lagging slightly relative to the velocity. A new friction model was incorporated into the model of the steering compensator and it was attempted to re-calculate the admittance function for the case of the SAE-10 oil. The result is shown in Fig. 23 where the improvement in the low-frequency phase characteristic is obvious.

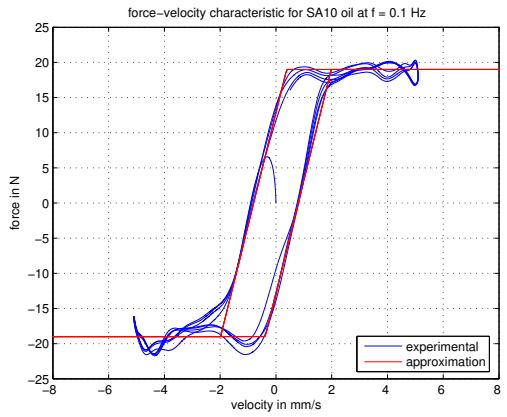

Fig. 22. The force-velocity characteristic for the SAE-10 oil at $f = 0.1$ Hz.

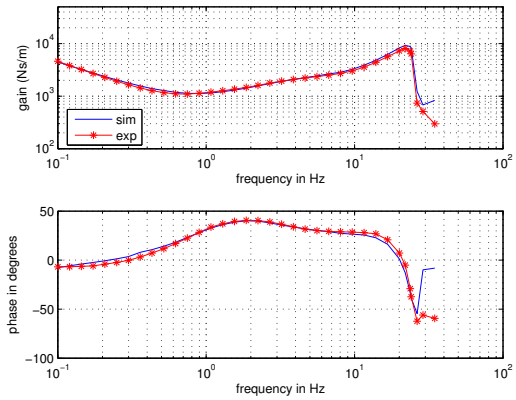

Fig. 23. Comparison of the admittance functions for the SAE-10 oil when using the refined friction model.

V. CONCLUSIONS

This paper has presented experimental results on the testing of a prototype mechanical steering compensator for motorcycles. The basic concept of the steering compensator design is that it performs as an inerter in series with a damper. The rationale for this is that the inerter has been shown to be stabilising for the weave mode in motorcycles while the damper is stabilising for the wobble mode. The mass of the prototype and the torque rating were both considered to be in a realistic range for possible practical application. This paper has studied whether the dynamic characteristics achieved by the device are sufficiently close to the required ones and has examined the nature and cause of perceived deviations.

In addition to the series combination of a damper and inerter the presence of a small parasitic inertance and a series compliance (spring) were expected in the device. Also, friction and backlash were expected. All these features were readily apparent in the experimental admittance function of the device. The presence of a hysteresis in the friction behaviour was also seen in the experimental data. To achieve a good fit between experimental data and model it was found advantageous to include a parasitic parallel linear damping term, which was not anticipated. The possible source of this damping effect is currently being investigated.

With all the above elements included in the model a very good fit was obtained with the time domain experimental data and there was also a good match with the experimental admittance function. The frequency response behaviour in the frequency range 1–20 Hz was broadly in line with that desired by the application, which we consider promising for possible practical application.

VI. ACKNOWLEDGEMENTS

We would like to thank David Cebon for making the Vehicle Dynamics Group's hydraulic ram available to us, and to John Beavis and Richard Roebuck for their assistance in the experiments.

REFERENCES

[1] S. Evangelou, D. J. N. Limebeer, R. S. Sharp, and M. C. Smith, "Control of motorcycle steering instabilities," *Control Systems Magazine, IEEE*, vol. 26, no. 5, pp. 78–88, Oct 2006.

[2] ——, "Steering compensation for high-performance motorcycles," in *43rd IEEE Conference on Decision and Control*, Bahamas, 2004.

[3] M. C. Smith, "Synthesis of mechanical networks: The inerter," *IEEE Transactions on Automatic Control*, vol. 47, no. 10, pp. 1648–1662, 2002.

[4] M. C. Smith and F.-C. Wang, "Performance benefits in passive vehicle suspensions employing inerters," *Vehicle System Dynamics*, vol. 42, pp. 235–257, 2004.

[5] C. Papageorgiou and M. C. Smith, "Positive real synthesis using matrix inequalities for mechanical networks: Application to vehicle suspension," *IEEE Trans. Contr. Syst. Technol.*, vol. 14, no. 3, pp. 423–435, 2006.

[6] M. C. Smith, "Force-controlling mechanical device," patent pending, Intl. App. No. PCT/GB02/03056, priority date: 4 July 2001.

[7] C. Papageorgiou and M. C. Smith, "Laboratory experimental testing of inerters," in *44th IEEE Conference on Decision and Control*, Seville, Spain, December 2005, pp. 3351–3356.

[8] D. J. N. Limebeer, R. S. Sharp, and S. Evangelou, "Motorcycle steering oscillations due to road profiling," *Transactions of the ASME, Journal of Applied Mechanics*, vol. 69, no. 6, pp. 724–739, 2002.

[9] L. Ljung, *System identification: Theory for the user*. Prentice Hall, 1987.

[10] M. Nordin, J. Galic, and P.-O. Gutman, "New models for backlash and gear play," *International Journal of Adaptive Control and Signal Processing*, vol. 11, pp. 49–63, 1997.